Hindawi
Geofluids
Volume 2023, Article ID 5534305, 18 pages
https://doi.org/10.1155/2023/5534305

Research Article

Production Forecasting of Unruly Geoenergy Extraction Wells Using Gaussian Decline Curve Analysis

Ruud Weijermars [1,2]

[1]*Department of Petroleum Engineering, College of Petroleum Engineering and Geosciences (CPG), King Fahd University of Petroleum & Minerals, Dhahran 31261, Saudi Arabia*
[2]*Center for Integrative Petroleum Research (CIPR), King Fahd University of Petroleum & Minerals, KFUPM, Dhahran 31261, Saudi Arabia*

Correspondence should be addressed to Ruud Weijermars; ruud.weijermars@kfupm.edu.sa

Received 7 February 2023; Revised 19 May 2023; Accepted 19 August 2023; Published 28 September 2023

Academic Editor: Shengnan Nancy Chen

Fast and rigorous well performance evaluation is made possible by new solutions of the pressure diffusion equation. The derived Gaussian pressure transient (GPT) solutions can be practically formulated as a decline curve analysis (DCA) equation for history matching of historic well rates to then forecast the future well performance and estimate the remaining reserves. Application in rate transient analysis (RTA) mode is also possible to estimate fracture half-lengths. Because GPT solutions are physics-based, these can be used for production forecasting as well as in reservoir simulation mode (by computing the spatial and temporal pressure gradients everywhere in the reservoir section drained by either an existing or a planned well). The present paper focuses on the physics-based production forecasting of so-called "unruly" wells, which at first seem to have production behavior noncompliant with any DCA curve. Four shale wells (one from the Utica, Ohio; one from the Eagle Ford Formation, East Texas; and two from the Wolfcamp Formation, West Texas) are analyzed in detail. Physics-based adjustments are made to the Gaussian DCA history matching process, showing how the production rate of these wells is fully compliant with the rate implied by the hydraulic diffusivity of the reservoir sections where these wells drain from.

1. Introduction

Recovery of energy from subsurface reservoirs has significantly shifted over the past two decades towards applying multistage fracturing technology to maximize the rate of fluid extraction [1]. However, operators of geothermal, oil, and gas wells still face challenges when appraising the expected ultimate recovery of future wells to be drilled [2, 3]. Many wells behave unruly (see Section 2.3), which is why appraisal is still a tedious undertaking, especially when needed for financing the cost of drilling and completing more new wells. The operator needs a high rate of cash from financing activities, because the operational income for many shale leases is insufficient to cover the cost of new wells to be drilled [4]. Companies listed on the New York Stock Exchange (NYSE) have the additional requirement of reporting compliance with SEC reserves reporting rules and guidelines, which means the proved reserves of both ruly and unruly wells in undrilled locations must be estimated using approved methods (either deterministic or probabilistic) for reserve estimation [5, 6].

To meet the requirement of reliable estimation of proved reserves and associated probable and possible categories, as well as the mandatory valuation of the net present value (NPV) of the proved reserves as per the reporting date (discounted at 10%, so-called NPV10 values), a variety of tools can be used for reserve estimation and production forecasting (in combination with discounted cash flow analysis). Two principal approaches can be applied: (1) phenomenological decline curve analysis (DCA methods) and/or (2) physics-based reservoir simulations. Both tool sets require the methods must history match certain reservoir and well performance data to calibrate the models and ensure the quality of the subsequent production forecasts and reserve

estimations will be meaningful. *Unruly* wells is a term introduced here to distinguish certain wells from *ruly* wells. For ruly wells, the production data can be immediately fitted with a variety of DCA methods, as well as history matched by a variety of numerical reservoir simulators. However, so-called unruly wells occur in many shale plays (see case studies in Section 3 of this paper) and can commonly not be fit simply by any method without amendments to the procedure.

The two principal classes of well performance evaluation methods commonly used are DCA and full reservoir models. The relative benefits and pitfalls of these methods have been extensively reviewed in prior work [1, 7–9]. While DCA methods are easy to use and fast in execution with negligible software license fees, traditional DCA methods are not physics-based and therefore unsuitable to predict how undrilled wells without production data will perform [10–12], especially when the design parameters of new wells to be drilled are to be improved. On the other hand, the more advanced physics-based simulators immediately are more complex to use, have higher license fees, and require more input parameters than just well production data to provide meaningful output [13]. As a result, most operators of geoenergy extraction wells today still predominantly rely on DCA methods for well performance forecasting and reserve estimation. They use reservoir simulations sparingly, usually only on a subset of wells for the acreage to be developed.

The main focus in this paper is on how a relatively new Gaussian DCA method (see Section 2.1) can be applied to accommodate history matches of unruly wells. Foremost, all DCA methods have great practical value because they can history match real-world well rate data from the past months to constrain the shape of a type curve, which can then be used to forecast the production rate of the well for future remaining months in the economic well life. The advantage is that no detailed reservoir data are needed to provide estimates for the remaining reserves from a given date forward. Combined with the historical cumulative production, DCA tools give acceptable results for the estimate ultimate recovery (EUR) of shale wells. As pointed out at length in prior work related to the Gaussian DCA method [14, 15], it differs from existing DCA formulas in that it is physics-based and only uses the hydraulic diffusivity as a matching parameter while resulting in excellent history matches. The appendix explains separately that the Gaussian DCA should ideally be applied to the total fluid produced. Exclusion of certain fluid volumes in wells producing liquids may lead to curve matches that appear poor, and this arises because the Gaussian method is physics-based and all fluid lifted by the well should be included and accounted for.

This paper highlights the strengths of the Gaussian solution of the diffusivity equation [14, 15], as a newly developed hybrid method for production forecasting and advanced reservoir modeling, which combines ease of use with fast results. Using the basic GPT methodology, the new case studies presented here highlight in detail how even the production behavior of so-called unruly wells can be readily described by the new production forecasting and reserve estimation method. Four such case study wells are analyzed, from three different US shale plays (one well in the Utica Formation, Ohio; one in the Eagle Ford Formation, East Texas; and two wells producing from the Wolfcamp Formation, West Texas). The solutions at the basis of GPT applications have been published in open source peer-reviewed journals [14, 15], due to which no license fees are due in principle. However, for corporate applications requiring a slick interface and back-office support, new products are under development accompanied by efforts to found an organization that can serve corporate clients and others as a non-for-profit foundation.

2. Methodology

This section briefly states the key equations (Section 2.1) and provides a brief overview of the GPT applications (Section 2.2). The final section explains the difference between *ruly* and *unruly* wells (Section 2.3). The remainder of this study (Sections 3 and onward) is dedicated to the fleshing out of what happens in such unruly wells and how Gaussian DCA can still be applied without any real impediments, once the root causes of the apparent unruliness have been explained.

2.1. Key Equations. The traditional well testing equation for a radial well is given by [16, 17]

$$q_W = [P_0 - P(r,t)]\frac{k}{\mu}\frac{2\pi h}{B}E_i\left(\frac{-r^2}{4D_h t}\right). \tag{1}$$

This solution used in well testing uses the (radial) pressure transient, $P(r,t)$, in the reservoir as a function of the estimated diffusivity, D_h, and an assumed constant well rate, q_W, as measured during brief flow tests. Ambient parameters are the formation volume factor, B; fluid viscosity, μ; permeability, k; initial reservoir pressure, P_0; payzone height, h; and well radius, r.

The recently derived GPT solution for a vertical well in radial coordinates is [15]

$$q_W(t) = \frac{(P_0 - P_{\mathrm{BH}})}{2D_h t}\frac{k}{\mu}\frac{2\pi h}{B}r^2 e^{-r^2/4D_h t} = \frac{(P_0 - P_{\mathrm{BH}})}{D_h t}\frac{k}{\mu}\frac{\pi h}{B}r^2 e^{-r^2/4D_h t}. \tag{2}$$

P_{BH} is the assumed constant bottomhole pressure in the well. Equation (2) is a drastic departure from the classical well testing Equation (1), because in the new solution of Equation (2), the well rate is not used (nor needed) to find the pressure advance. Reconciling the well test Equation (1) and the new GPT solution of Equation (2) is not possible: the GPT solution assumes as a constant P_{BH} through the well life, while the well test Equation (1) assumes the P_{BH} drops according to $P(r,t)$. However, the GPT solution can solve for the spatial and temporal pressure transient advance everywhere in the reservoir.

The shape of the pressure transient advance is controlled by the shape of the source (Figure 1). As the flow is into the

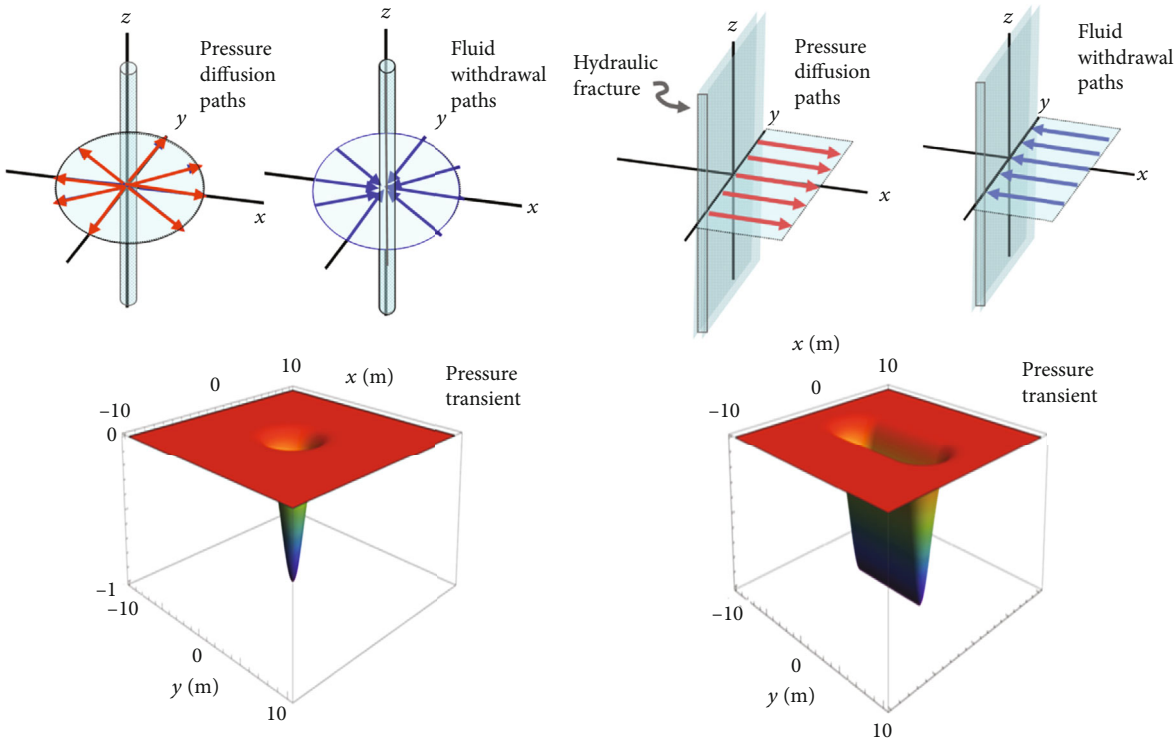

(a) Well = cylindrical source

(b) Fracture = planar source

FIGURE 1: Two fundamental modes of pressure diffusion occur in well systems. (a) 2D diffusion prevails in vertical wells. (b) 1D diffusion prevails in hydraulically fractured well systems.

fracture surface from both sides, we can translate Darcy flux q_D into well head rate using $q_w = 2A(q_D/B)$ with single-sided fracture area A and formation volume factor B. For the 1D diffusion of a pressure change imposed on a reservoir region by a hydraulically fractured well system, the well rate is then given by the following equation [15]:

$$q_w(t) = 2nY_f h \frac{k}{\mu B} \frac{P_0 - P_{BH}}{D_h t} x e^{-\left(x^2/4tD_h\right)}. \quad (3)$$

We only consider the half-length Y_f of the fracture that is effectively propped (Figure 2), such that approximately infinite conductivity is achieved. The well rate is computed based on influx at $x = 1$ unit length from the diffusion source.

In case field units are used as inputs, as is the case in US petroleum industry, one needs to make sure to use Equation (3) with the following conversion factors:

$$q_w(t) = \frac{C_1 C_2}{C_3} \frac{2nhkY_f(P_0 - P_{BH})}{\mu B D_h t} x e^{-x^2/4D_h t}. \quad (4)$$

The conversion factors have the following values:

$C_1 = 0.178108$ bbls/ft^3. This factor arises because the input units in feet on the right-hand side lead to cubic feet, which needs conversion to oil bbls (for subsequent multiplication with the volume factor in bbl/stb to end up with stb for the left-hand side well rate). The required conversion factor is 1 ft^3 = 0.178108 bbls. If we work with gas wells, the conversion factor $C_1 = 0.001$ Mcf/ft^3, because 1 ft^3 = 0.001 Mcf, and the produced gas volume will be expressed in Mcf.

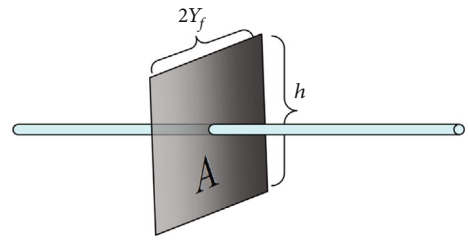

FIGURE 2: Principle sketch showing the fracture area (A) that is effectively propped is given by the product of twice the fracture half-length and the height of the payzone.

$C_2 = 1.06235E - 14$ ft^2/mD. This factor is needed to convert square feet units of permeability and prorated for inputs in mD. The required conversion factor is 1 mD = 1.06235×10^{-14} ft^2.

$C_3 = 1.67868E - 12$ psi·day/cPoise. This factor is needed if the viscosity input is in cPoise; then, conversion of viscosity to psi·day will result in output for well rate in stb/day. The required conversion factor is: 1 cPoise = 1.67868×10^{-12} psi·day.

Another major step for the purpose of the current analysis is to assume the initial well rate q_i starts when the initial

Table 1: Practical applications of GPT-based solutions.

Applications	Key references
Hydraulic diffusivity estimations for shale formations	[18, 19]
Probabilistic reserve estimation and production forecasting	[18]
Establishing relative importance of molecular and pressure diffusion in shale	[19]
Quantifying stress reversals during hydraulic fracturing	[*]
Computing surface uplift during CO_2-sequestration in subsurface reservoirs	[*]
Computing flow paths in the drained reservoir space	[*]
Estimation of fracture half-lengths	[*]
Computing and visualizing pressure interference effects due to fracture spacing and well spacing reduction	[*]
Shale acreage development optimization based on full field model	[*]

[*] References removed on request of publisher to reduce self-citations.

time $t = t_1$ expended the first unit of time (for example, 1 day in the case of daily production rates, as was used in all the case studies of this paper) and is given by [15, 18]

$$q_i = 2nY_f h \frac{k}{B\mu} \frac{P_0 - P_{\mathrm{BH}}}{t_1 D_h} x e^{-\left(x^2/4t_1 D_h\right)}. \tag{5}$$

Taking the ratio of Equations (3) and (5) gives [15, 18]

$$q_w(t) = q_i \frac{t_1}{t} e^{\left(x^2/4D_h\right)\left((1/t_1)-(1/t)\right)}. \tag{6}$$

Equation (6) can be normalized using $t' = t/t_1$ and $D_h{}' = D_h t_1/x^2$ to give [15, 18, 19]

$$q_w(t) = q_i \frac{1}{t'} e^{\left(1/4D_h{}'\right)\left(1-\left(1/t'\right)\right)}. \tag{7}$$

The Gaussian DCA solution can conveniently start with $q_i = 1$ production unit/day and then adequately solve for the hydraulic diffusivity, D_h, by history matching the daily production data of a well. The asterisked values in Equation (7) can be readily dimensionalized, because 1 nondimensional length unit is equal to 1 dimensional length unit. Likewise, 1 nondimensional diffusivity unit is equal to 1 dimensional diffusion unit.

2.2. Principal Applications. The Gaussian method has been validated and deployed in a variety of detailed topical studies ranging from basic DCA applications [18, 19] to coupled models requiring the pressure transient as an informer of the local pressure state with consequent geomechanical response, such as principal stress reversals during hydraulic fracturing, surface uplift during fluid injection (including applications in carbon dioxide-sequestration projects), and surface subsidence due to fluid extraction from subsurface reservoirs. Table 1 lists the topics where GPT-based solutions have been implemented in practical applications.

2.3. Unruly Wells. The main focus of the present study is to analyze in detail how GPT-based Gaussian DCA can still be applied to fluid extraction wells with apparently "unruly" production performance. To clarify what is meant by such "unruly" wells, Figure 3 shows the historic production rate evolution for a "ruly" well, without any major operational noise. The Gaussian DCA curve (or any other DCA curve by other methods) can closely match the historic data of such wells. Our previous work has demonstrated how the Gaussian DCA method is both more accurate and faster than any other traditional DCA method, especially because early production data are honored. The Gaussian DCA method is physics-based, unlike the other DCA methods, and has been tested on numerous *ruly* shale oil and shale gas wells in recent studies [18, 19].

However, *unruly* wells typically behave as in Figure 4, where the irregular and volatile trend in the time series of the production data seems to initially preclude a close DCA curve match. The remainder of this study is aimed at showing how such unruly wells can still be adequately described by Gaussian DCA, provided that one takes into account some corrections for the operational effects causing the (apparent) unruliness of the production rate trend.

3. Gaussian DCA Applied to Unruly Wells

In an effort to refine the Gaussian method, this section presents a series of brief case studies of wells that at first appear less conformal to DCA matches when analyzing their historic production data. However, after a detailed assessment of the well data, one can readily explain how these wells can still be history matched with the Gaussian DCA method, in spite of the initial impression of apparently "unruly" behavior of these wells. Concluding that these wells would be "unsuitable" for Gaussian DCA history matches would be technically incorrect. The wells studied show that valuable data can indeed be inferred from these apparently unruly wells, like from any other—initially more conformal appearing—hydraulically fractured well. Four shale wells are analyzed in details: one from the Utica, Ohio (Section 3.1); one from the Eagle Ford Formation, East Texas (Section 3.2); and two wells from the Wolfcamp Formation, West Texas (Section 3.3). Physics-based adjustments are made to show how the flow behavior of these wells is fully compliant with the hydraulic diffusivity and Gaussian DCA method of the reservoir sections where these wells are drained from.

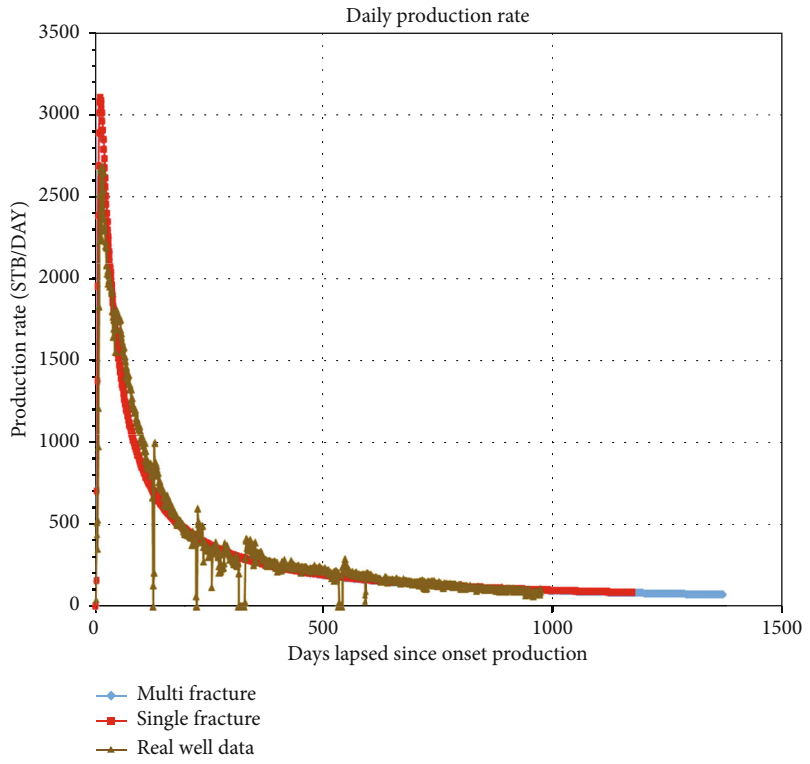

(a)

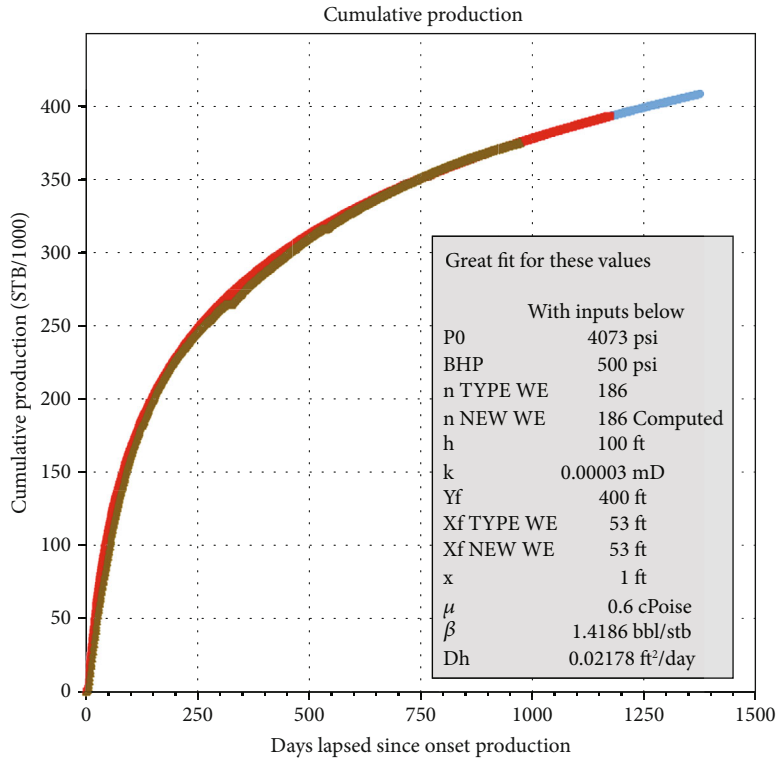

(b)

Figure 3: Ruly well with typical steady decline in historic daily production rates (a), which can be snuggly matched with Gaussian DCA curve. Similarly, the historic cumulative production of the well (b) can be tightly matched with the Gaussian DCA method. Historic data plotted are from Well U4 in the hydraulic fracturing test site (HFTS-1) in the Permian Basin.

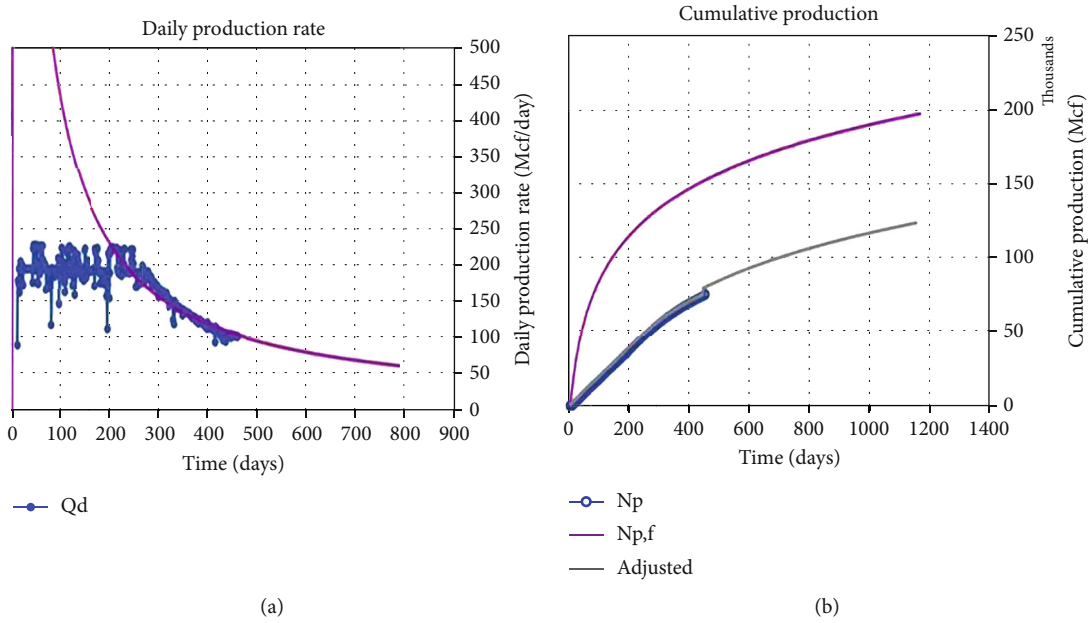

Figure 4: Unruly well with typical unsteady decline in the historic daily production rates (a), which cannot be snuggly matched with Gaussian DCA curve. Similarly, the historic cumulative production of the well (b) shows a vast overmatching if left uncorrected. Historic data plotted are from Well H2 in the Utica shale formation, Ohio.

3.1. Dry Gas Well Case Study—Utica Formation (Ohio). The Utica shale is a dry gas play in the state of Ohio, US [20, 21]. Analysis of daily production data from one of five subparallel parent wells completed from the same well pad reveals how operational issues may affect the history matching of such wells. For example, the DCA match to the historic production data for a central shale gas well (Figure 4) at first appeared as apparently a very poor match.

Close inspection of the daily production data reveals that during the first 250 days of production, the well rate of Well 2H appears to be artificially constrained by the production system. In fact, the operator reported that the production (initiated in Q2-2016) for the 5 wells combined was initially constrained to ~6200 Mcf/day [20]. Figure 5(a) annotates for the specific well how the production rate was constrained to 200 Mcf/day, neglecting the operational noise in the data causing the wriggling.

Fitting the Gaussian DCA curve to the daily production data after about day 250 (when the well was put on constant BHP control) honors the boundary assumption of a constant BHP for the Gaussian well model [14]). In fact, the Gaussian DCA curve (Figure 5(a)) shows how the well would have behaved during the first 250 days of production without the choking constraint on the production system, assuming the BHP would have been rapidly established to its later constant value. However, in reality—and due to the choking—the well only reached the constant BHP later in the first year of operation (Figure 6). The smooth BHP profile indicates that the well did not suffer from any operational complications.

Other reasons for the early plateau in the well rate, rather than facility constraints, could have been natural choking due to selection of a small tubing size or a maximum choke diameter limiting critical gas flow velocities, but this is not the case for the production system of the well in Figures 5(a) and 5(b). Completion limitations on maximum drawdown (initial reservoir pressure, sand production, gravel packs, etc.) are not involved either. Another motivation for manual choking could be avoidance of flaring and profound delay in gas sales due to low gas prices, but this did not apply to this well either. The main reason for choking at the well head was the limited compressor capacity of the separator unit on the well site.

The evident plateau in the early daily production data (Figure 5(a)) can at first be neglected for the Gaussian DCA fit but then needs to be reimported to correct for the downward shift in the actual cumulative production profile (Figure 5(b)). A realistic and accurate cumulative production profile can still be predicted with the Gaussian method by shifting the Gaussian cumulative downward (grey curve in Figure 5(b)), simply by using for the first 250 days the actual production data (not using the Gaussian cumulative that shows how the well would have behaved without the constraint on the production system). This approach gives the adjusted (grey curve) cumulative forecast (Figure 5(b)).

When applying Arps to history match such data, the first 250 days would also have to be unweighted to obtain meaningful forecasts. However, the advantage of using the Gaussian DCA method over Arps' method is that the former uses only one unknown parameter (the hydraulic diffusivity) in the history match to the actual well rates. The hydraulic diffusivity can be readily determined by history matching the production data as shown in Figure 5(a), which then provides a sound basis for reliable production forecasts and EUR estimations (Figure 5(b)) over the remaining well life. Moreover, the Gaussian DCA method is founded in reservoir physics (movement of the pressure transient) and can be readily applied in forward models to constrain the

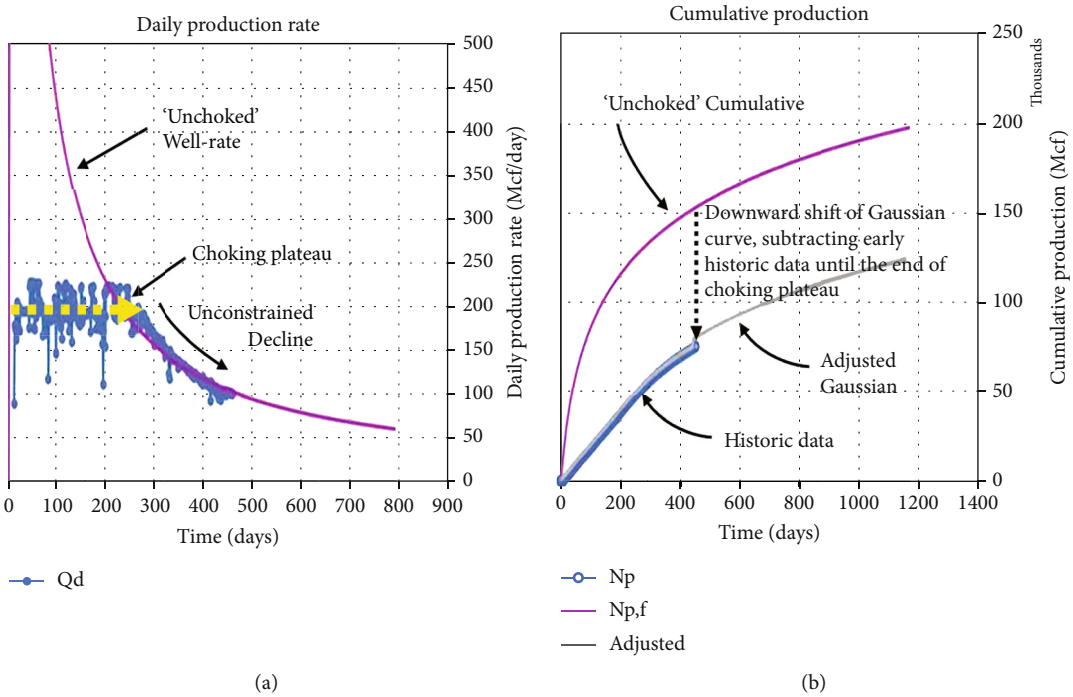

FIGURE 5: (a) Daily production rate of gas in Well H2, Utica shale formation, Ohio. Facility constraints choke the early well rate (blue dots), capping the gas flow during the first 250 days of production to 200 Mcf/day (yellow plateau). The Gaussian DCA curve can be fit snuggly (purple curve) using Equation (7) in least square error regression fit to the historic production data for the unconstrained decline after 250 days of production (blue points). (b) The cumulative production plot serving as a basis for estimation of ultimate recovery (EUR) and reserves. The Gaussian DCA curve (purple) is too high but can match the early production data (blue curve) and predict the forward trend after a simple adjustment (grey curve).

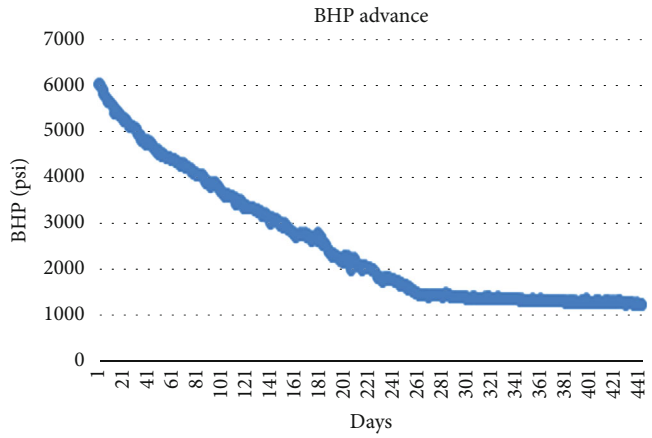

FIGURE 6: Pressure drop (BHP) in the case study well of Figures 5(a) and 5(b).

fracture half-lengths, after first determining the hydraulic diffusivity for the reservoir section of interest with the Gaussian DCA method.

History matching well rates with a reservoir simulator suggested that in case an arbitrary high permeability of 850 nD is adopted, the fracture half-length would be 75 ft; for lower adopted permeability of about 25 nD, the fracture half-length would be longer [21].

3.2. Black Oil Well Case Study—Eagle Ford Formation (East Texas). Another shale well, from the black oil maturity window in the Eagle Ford shale formation, was analyzed in detail because it exhibited a seemingly imperfect DCA fit (Figure 7). The well of concern is located in leasehold owned by the Texas A&M University System. The production performance and recovery rates of this well (Well H1) and nearby wells in the same leasehold have been extensively studied in prior work by our group. For further details, see [22].

Figure 7(a) shows the least square error fit of the Gaussian curve on 48-month historic production data. All daily data are used as provided by the operator; the incident of a negative well rate at day 400 of production (Figure 7(a)) likely was a malfunction of the data transmission. Nonetheless, the corresponding Gaussian fit on the cumulative

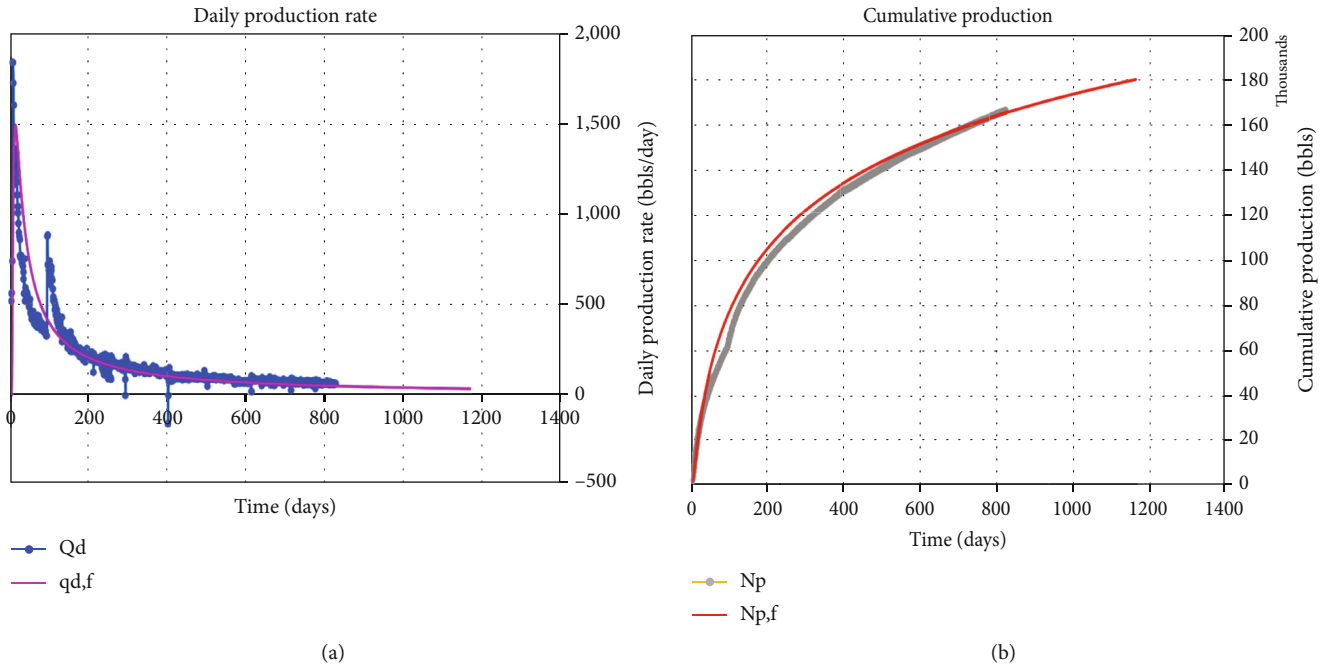

Figure 7: (a) Daily production data in shale oil Well H1, Eagle Ford Formation, Brazos County, East Texas. Gaussian DCA regression curve (purple) fit on the historic production data (blue dots). (b) Corresponding cumulative production curves.

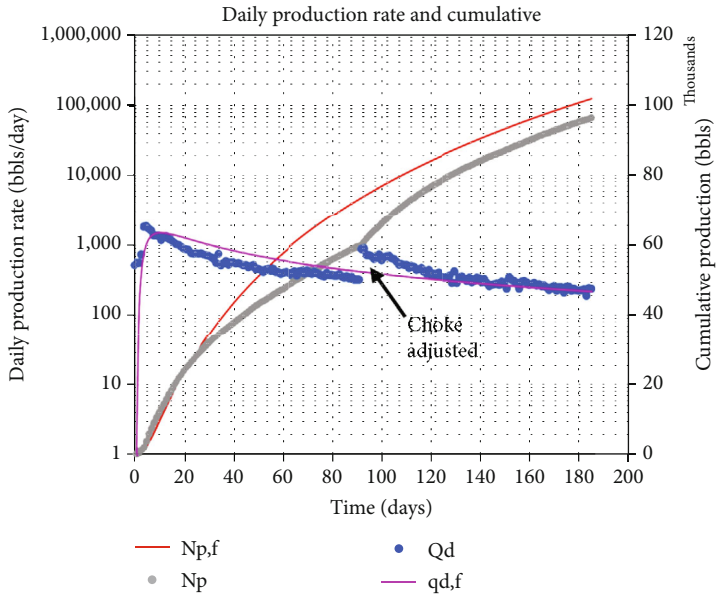

Figure 8: Magnified graph for Well H1 (Eagle Ford) with daily production data (blue) and Gaussian DCA curve (purple, left-hand scale). Cumulative is given for actual data (grey curve) and long-term Gaussian DCA fit (red, right-hand vertical scale).

production data (Figure 7(b)) seems reasonable, albeit slightly overmatching the actual cumulative production curve (grey, Figure 7(b)). The region where the mismatch is largest occurs during the first 200 days of production and is magnified in Figure 8.

Careful inspection of Figure 8 shows that a jump in the daily rate of production occurs after 90 days after the earlier production developed premature decline in the well rate. The premature decline in the well rate is reflected in the grey curve (actual cumulative production) which is overmatched by the Gaussian cumulative (red curve, Figure 8) as was already apparent in Figure 7(b).

If we next inspect the well report in detail, it appears that there was an adjustment in the choke setting precisely at day 90 of production, as is seen in the plot of Figure 9, which plots original daily production volumes and the tubing head pressure on the same timescale. The abrupt drop in tubing pressure at day 90 is now recognized as being caused by a manual adjustment of the choke setting from 18/64″ to 30/64″. Notwithstanding the occurrence of overestimation for

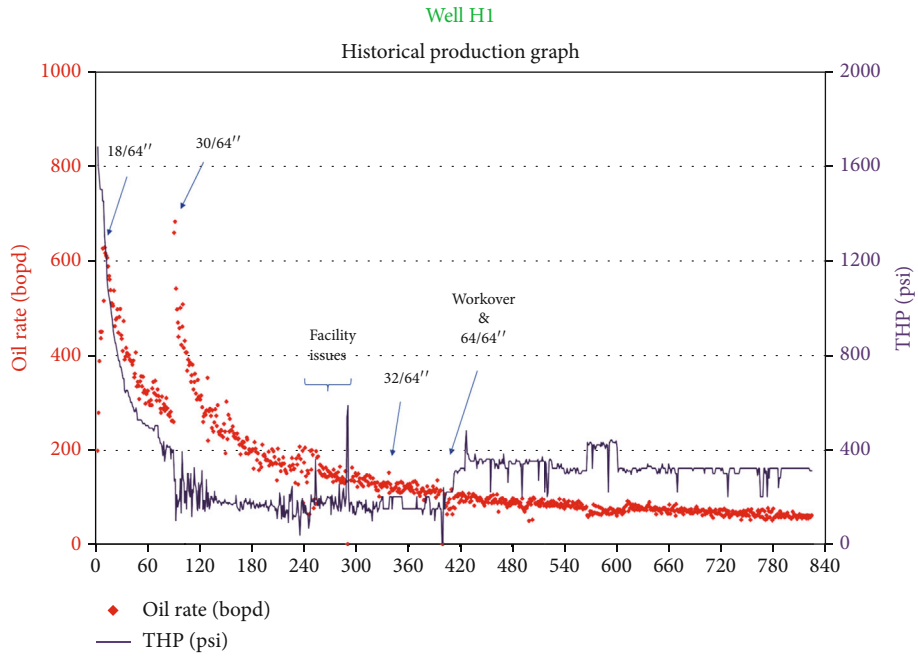

Figure 9: Detailed analysis of operational adjustments made by operator on Well H1 (Eagle Ford Formation) during the first two years of production.

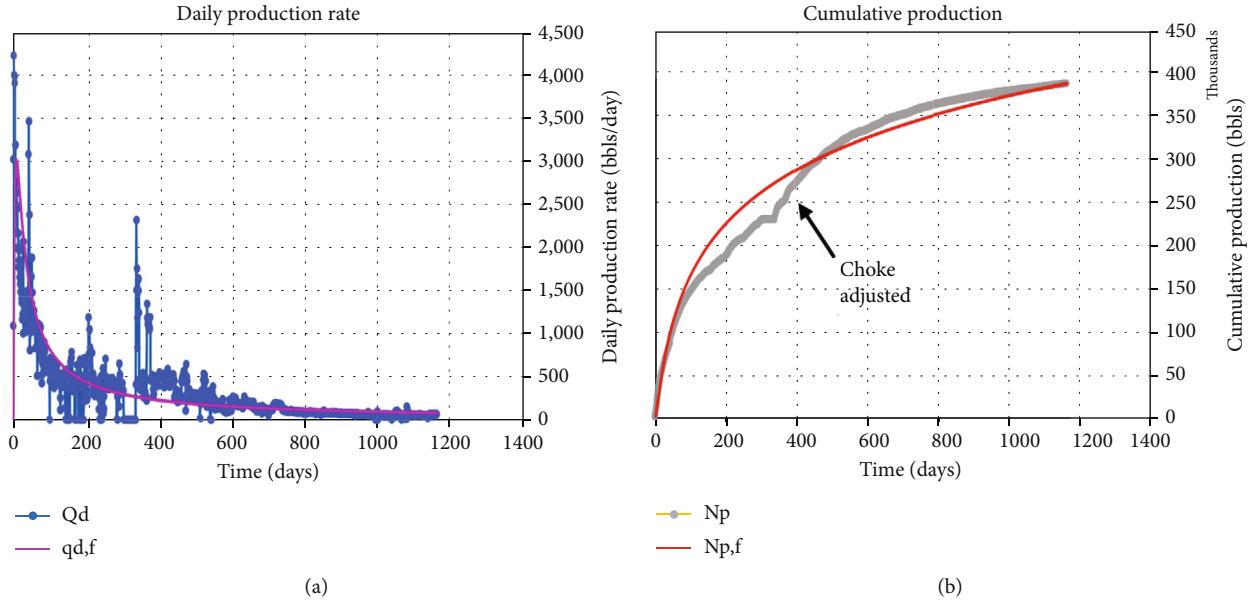

Figure 10: (a) Daily production data (blue) and Gaussian DCA regression curve fit (purple) for Well 4H, Wolfcamp Formation, Permian Basin. (b) Cumulative plot wit actual data (grey curve) and Gaussian regression fit (red curve), revealing mismatch of slightly unruly well.

the cumulative due to the early choke constraints, the Gaussian fit shown in Figure 7(b) is assumed to give reliable long-term performance data. Additionally, the estimated hydraulic diffusivity is assumed to be a characteristic for the reservoir section drained by the well.

3.3. Volatile Oil Well Case Study—Wolfcamp Formation (West Texas). A shale well from leasehold by the Texas Permanent University Fund in the Permian Basin (West Texas) was analyzed in detail in a prior study [23]. Here, we history match the production data of this key well for the first time with the Gaussian DCA method. The daily production data (Figure 10(a)) shows a sudden jump at day 350 of production similar to what was seen in the well of Figure 4(a) at day 250 of production. Likewise, the cumulative history match shows overmatching after the excellent match on the first hundred days of production (Figure 10(b)). The overmatch can be seen in detail in Figure 11.

The premature production decline seen during the early days of production of Well 4H can again be attributed to a

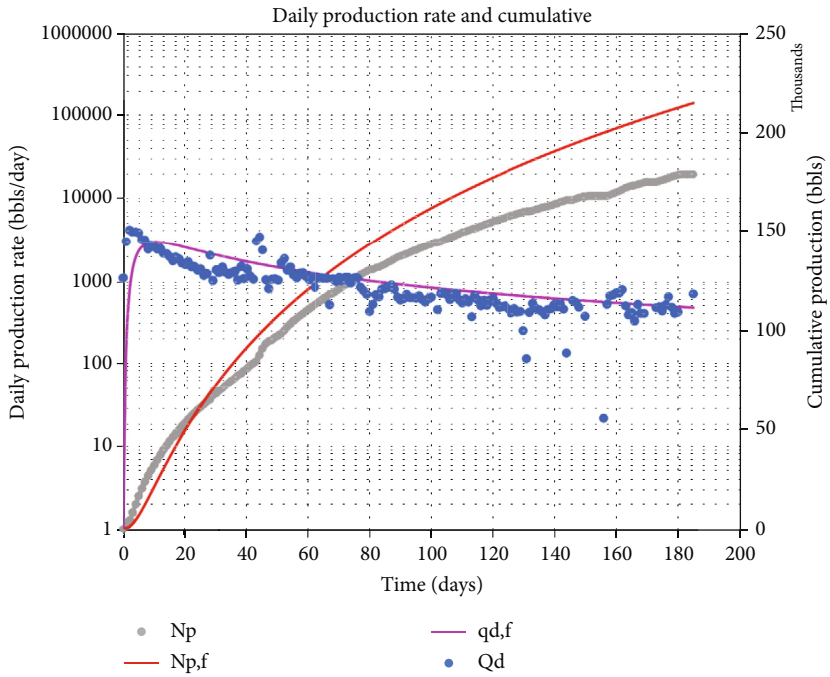

Figure 11: Magnified portion of production plots for Well 4H, showing only the first 200 days of production, with daily data (blue), Gaussian DCA regression curve (purple, left scale), and cumulative actual data (grey curve) and Gaussian fit (red curve, right-hand scale).

suboptimal choke setting. This means the Gaussian curve shows that the production that could have been realized was the choke setting not constraining the well rate. Adjustment of the choke setting after a brief period of well shut-in for pressure communication tests was reported by the well operator and explains the attenuation of the well rate seen in both the daily (Figure 10(a)) and cumulative production plot (Figure 10(b)). In spite of the imperfect match of the Gaussian cumulative and the actual well rate, the mismatch can be entirely attributed to the well interventions.

A second well studied, also from the oil maturity window in the Wolfcamp Formation (West Texas), was part of the HFTS-1 field experiment of the US Department of Energy. This was the only well out of the eleven wells matched with the Gaussian DCA in a prior study [18] that did not allow for a near-perfect history match (Figures 12(a) and 12(b)). The other 10 wells matched very closely the original production data [18].

The daily production of HFTS-1 Well U8 could not be matched snuggly by the Gaussian curve using any *constant*-valued hydraulic diffusivity (Figures 12(a) and 12(b)). However, if the diffusivity was allowed to behave *time-dependent*, the Gaussian DCA curve will closely match to the historic production data (Figures 12(c) and 12(d)). The residual overmatch of the cumulative is due to the peak rate at early times in the Gaussian curve, but which was not occurring in reality (due choke settings and other operational constraints). The Gaussian curve (Figures 12(a) and 12(b)) simply shows what would have been the well's performance without operational constraints.

The time dependency of the hydraulic diffusivity is accounted for (Figures 12(c) and 12(d)) by introducing fractional decrease of its value with time. The physical mechanism responsible for the reduction of the hydraulic diffusivity is in this well assumed to occur due to chemical scaling processes. Note that the residual overmatch in Figures 12(c) and 12(d) could be corrected for applying the same curve shifting procedure using actual production data for early time as described for the well of Figures 5(a) and 5(b).

4. Discussion

4.1. Gaussian DCA in Unruly Wells. The production performance of oil and gas wells with unsteady production rate data that could not be matched with Gaussian DCA curves without adjustments (so-called unruly wells) has been analyzed in detail. From this analysis, it became apparent how big the impact on cumulative production is when the well rate is constrained not by the reservoir deliverability (succinctly captured by the hydraulic diffusivity) but by operational constraints (such as natural and or manmade choking in the production system). In one well, time dependency of the hydraulic diffusivity was inferred to occur, because otherwise the historic production data could not be matched. The time dependency was assumed to be due to formation damage caused by scaling. Another potential cause could be the extensive treatment with radioactive tracers injected in this particular well.

One may conclude that the hydraulic diffusivity of the reservoir section to be drained is a powerful and succinct predictor of how a shale well (or a well in any other porous rock formation) will perform. The hydraulic diffusivity represents how geology shaped the pore space connectivity (permeability), storativity (porosity), and matrix compressibility, as well as capturing the nature of the hydrocarbon maturation process (fluid viscosity and fluid compressibility.

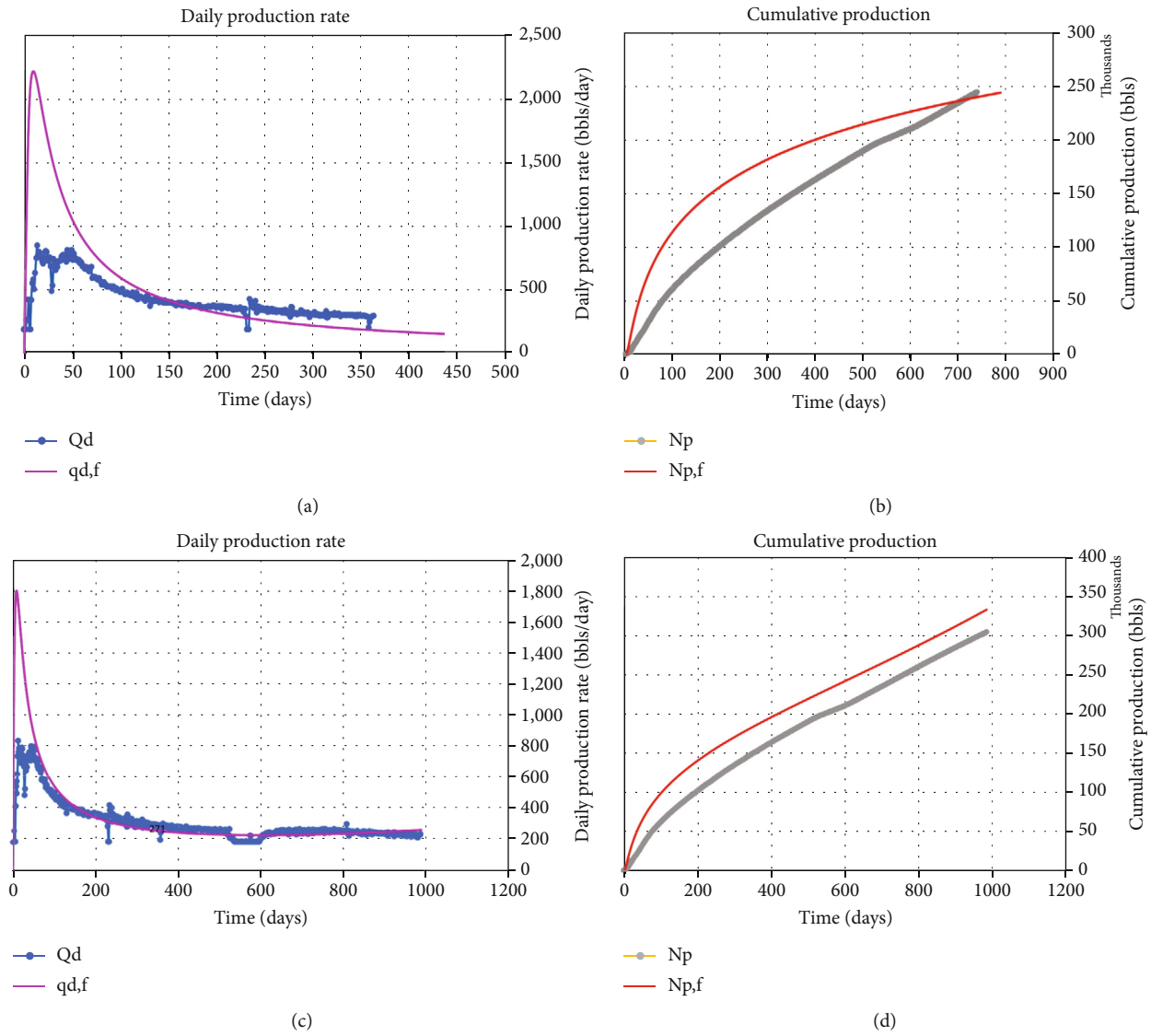

Figure 12: Production analysis plots for Well U8, HFTS-1 (Wolfcamp Formation, Permian Basin, West Texas). Neither daily (a) nor cumulative plot (b) can be matched by the Gaussian DCA regression curve when a fixed value is used for the hydraulic diffusivity. (c, d) Reasonably snug fit becomes possible using time-dependent diffusivity. Overfitting in (d) due to early peak mismatch attributed to production system choke can be adjusted using the procedure described in Figure 5(b).

Table 2: Wells with hydraulic diffusivity estimations based on history matching in this paper.

Well name	Formation	County	Hydraulic diffusivity field units ($ft^2 \cdot day^{-1}$)	Hydraulic diffusivity SI units ($m^2 \cdot s^{-1}$)	Figure number
HFTS-1-U4	Wolfcamp	Reagan, TX	0.02178	2.34×10^{-8}	1
2H	Utica	Harrison, OH	0.02320	2.49×10^{-8}	2
H1	Eagle Ford	Brazos, TX	0.02340	2.52×10^{-8}	7
4H	Wolfcamp	Upton, TX	0.02182	2.35×10^{-8}	10
HFTS-1-U8	Wolfcamp	Reagan, TX	0.0230 (max)	2.47×10^{-8}	12

If the well draining the reservoir is underperforming, one cause may be the overall diffusivity is rather low. Our history match estimations of the hydraulic diffusivity for each of the unruly wells are summarized in Table 2. These values are close to those estimated in our previous work for ruly shale gas wells [19] and black oil wells [18].

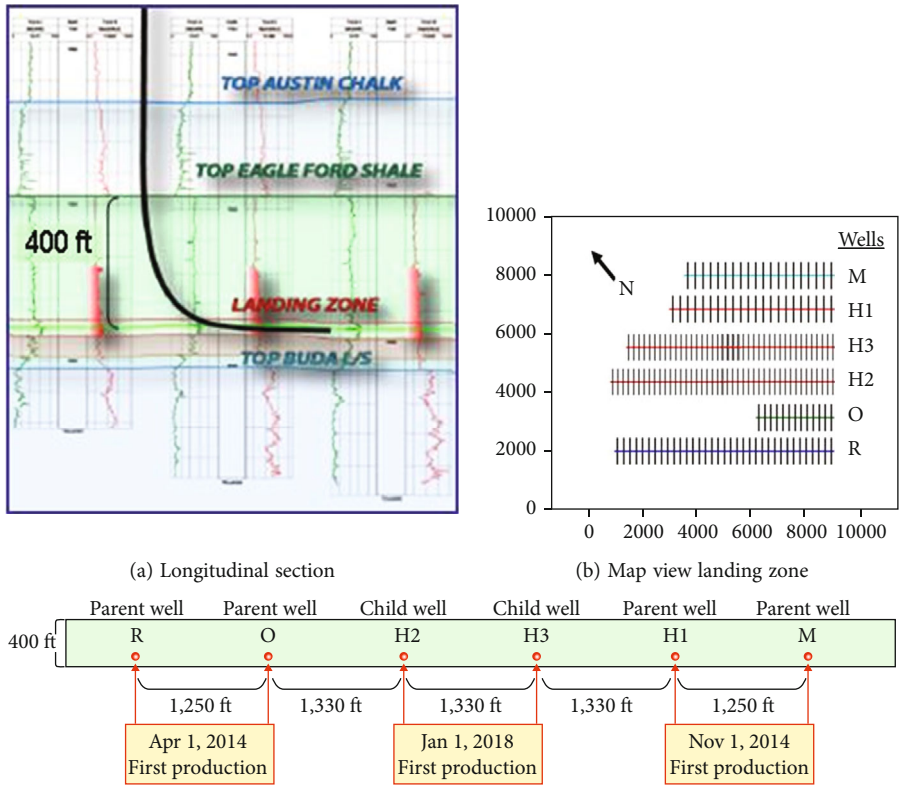

Figure 13: Layout of case study wells: (a) longitudinal section of typical wellbore in the Eagle Ford landing zone; (b) map view showing the lateral extend of the 4 parent wells (R, O, H1, and M, completed in fall 2013) and 2 infill (so-called child) wells (H2 and H3, completed in fall 2017); (c) gunbarrel view of the 6 wells.

4.2. Operational Recommendations. Separately, our evaluation of unruly wells reveals how important operational excellence is. The suboptimal well rate early in a well's history is profoundly impacting the cumulative production volume, which will reduce the net present value and internal rate of return of the well. This should be avoided at all times (unless the operator has deliberate reasons to choke the well due to separator capacity limits, or the wish to delay production sales when low product prices would render a well subeconomic). If occurring unplanned, a review of the well design and choke optimization procedure is highly recommended to avoid undue loss of future revenues.

5. Conclusions

This study made a distinction between rule and unruly shale wells, based on production analysis criteria. Ruly wells exhibit little operational noise and their production data can be readily matched by a variety of established history matching tools. However, unruly wells, with apparently irregular and volatile trend in their production profiles, have long been discarded as being either ill-suited or unsuitable for production analysis with traditional methods. This poses a problem for operators of shale acreage, because such wells are frequently encountered.

A new, fast method based on a new solution of the pressure diffusion equation, termed the Gaussian pressure transient (GPT) solution, gives reasonable regression fit curves on both ruly and unruly shale wells. This assertion was substantiated in this study after analyzing the production data of four unruly shale wells, sampled from three major US shale plays (Eagle Ford, Utica, and Wolfcamp Formations). By demonstrating the effective use of the new GPT-based solutions the Gaussian DCA mode (and highlighting other possible application modes, see Table 1), the hope is this perspective paper will accelerate the dispersion of the new method in both industry for operational applications and in research institutions for continued validation.

Appendix

Gaussian DCA History Matches on Total Fluid Production versus Oil Only

The Gaussian DCA should ideally be applied to the total fluid produced. Exclusion of certain fluid volumes produced leads to curve matches that may appear poor. The reason being that the Gaussian method is physics-based, so all fluid lifted by the well should be included and accounted for. Examples of how the matches may appear poor at first are given here using four parent wells from an Eagle Ford lease [22]. The relative position of the parent wells is given in longitudinal vertical section view, well map, and gunbarrel

Table 3: Effective lateral length, fracture spacing, fracture number, and total proppant injected for the Eagle Ford field data.

Well name —	Effective lateral length ft	Number of completion stage —	Completion stage spacing ft	Number of fractures —	Fracture spacing ft	Total proppant lbs
R	8,630	35	250	139	63	12,282,550
O	2,942	13	240	52	60	4,090,160
H1	6,550	22	300	131	50	10,664,970
H2	7,905	51	45-180	433	18	
H3	7,359	50	56-177	413	18	
M	5,950	20	300	119	50	9,398,600

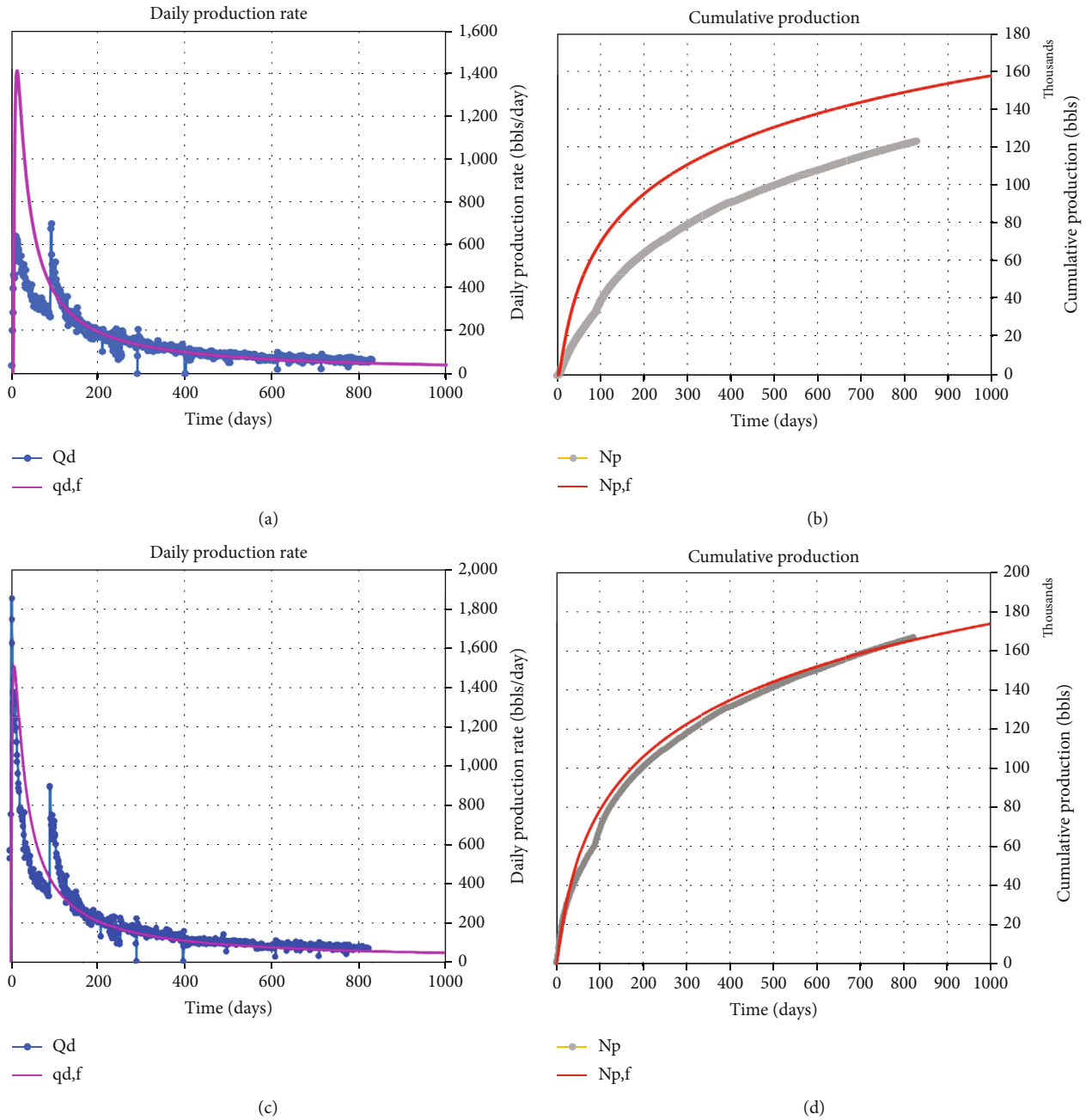

Figure 14: Well H1: (a) Gaussian match on historic daily oil rate only; (b) corresponding match on cumulative oil production; (c) improved Gaussian DCA match on total fluid produced; (d) corresponding match on cumulative production data (total fluid).

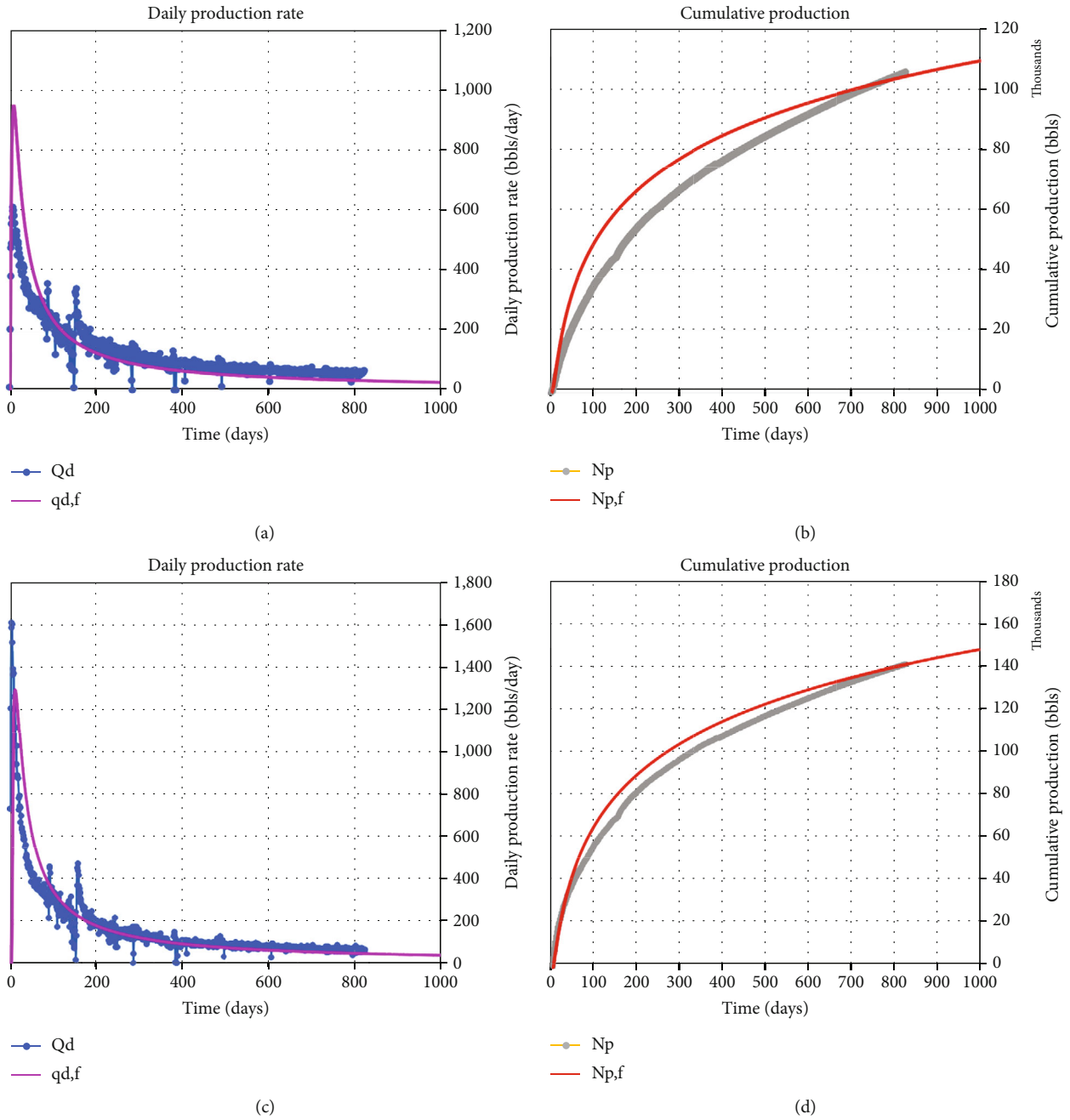

Figure 15: Well M: (a) Gaussian match on historic daily oil rate only; (b) corresponding match on cumulative oil production; (c) improved Gaussian DCA match on total fluid produced; (d) corresponding match on cumulative production data (total fluid).

views of Figure 13. The basic completion attributes are summarized in Table 3.

The historic daily rates and cumulative for each of the four wells (Well H1, M, R, and O) were first matched using oil production rates only, and then, improved Gaussian DCA history matches were possible when the total fluid production was used (Figures 14–17). The hydraulic diffusivity are given in Table 4, which were established using least square error fits, with Excel's goal seek function, altering the diffusivity until the optimum matches were obtained. The graphical matches are given in Figures 14–17 and explained in some detail below.

The daily and cumulative historic production data of Well H1 matched with Gaussian DCA, initially using oil production rates only (Figures 14(a) and 14(b)). Visual inspection suggests that the Gaussian DCA curves give poor matches. However, if we use water and oil production rates combined, the matches improve substantially and appear satisfactory (Figures 14(c) and 14(d)). Close matches of the historic production date thus appear possible with the Gaussian DCA, in spite of the well having choke setting adjustments after 90 days of production that would jeopardize DCA match quality of most other DCA methods. Well H1 is discussed in some more detail in Figures 7–9 of the

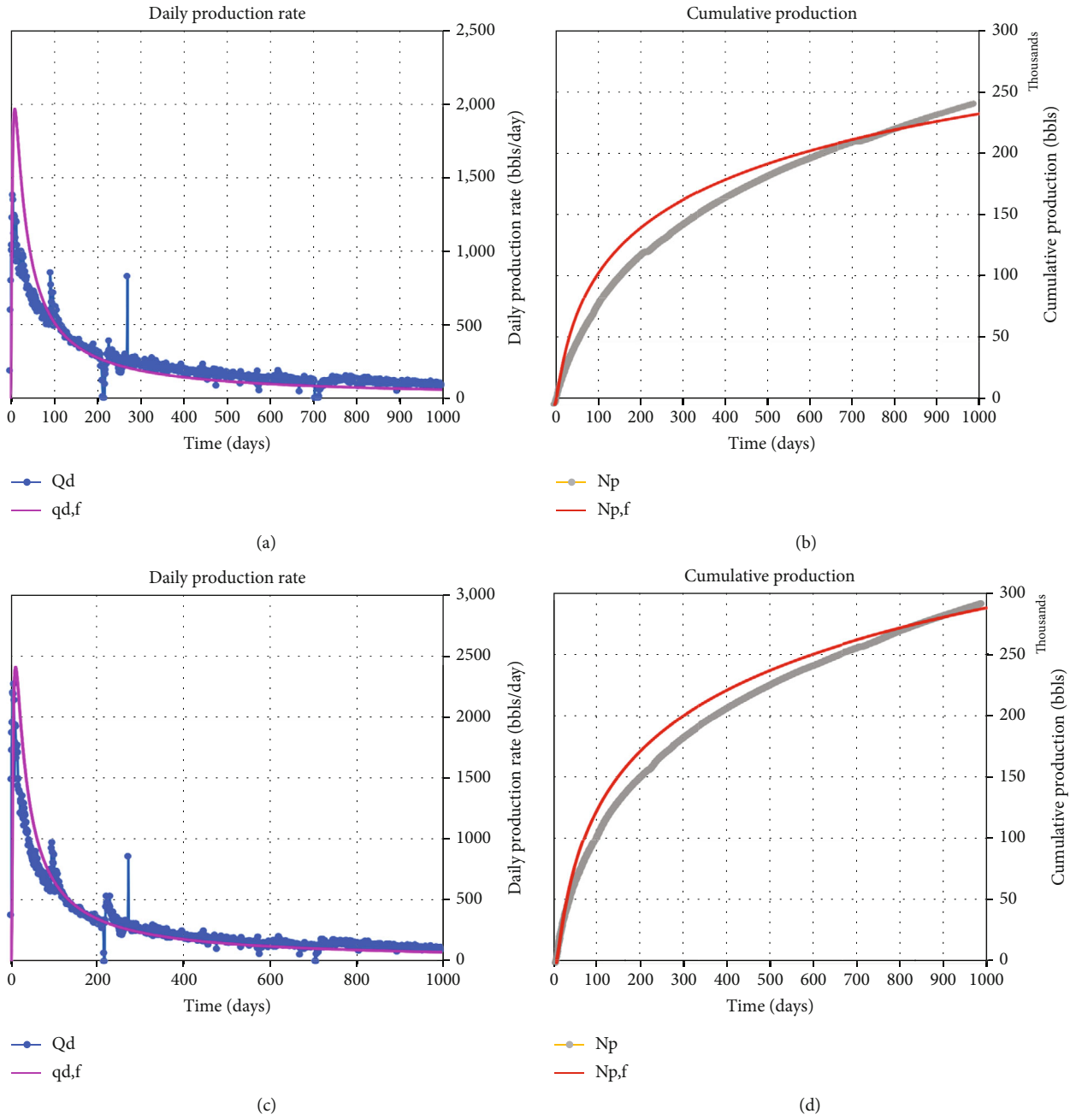

Figure 16: Well R: (a) Gaussian match on historic daily oil rate only; (b) corresponding match on cumulative oil production; (c) improved Gaussian DCA match on total fluid produced; (d) corresponding match on cumulative production data (total fluid).

main text. Note that the single day negative data point (due to a meter transmission error) shown in Figure 7 has been removed in the analysis of Figures 14 and 15.

The other three parent wells were also subjected to the same analysis, comparing the history match quality using partial (oil only) with those obtained using total fluid production volumes. Figures 15(a)–15(d) show how the history matches on Well M daily and cumulative historic production data improved when the total well rates were used. The total daily fluid rates and cumulative production can be matched snugly with the Gaussian DCA curves (Figures 15(c) and 15(d)). However, if oil rates only are used, the matches appear poor (Figures 15(a) and 15(b)). The reason is that early in the well life, there is significant water production (partly retarded flowback water), such that matching of the oil rates only, using a single diffusivity throughout the well life, results in the poor matches, especially early in the well life (Figure 15(a)).

Figures 16(a)–16(d) show how the history matches on Well R production data also improved substantially when total well rates were used. The historic total daily fluid rates and cumulative production can be matched snugly (Figures 15(c) and 15(d)). However, if only oil rates and cumulative historic production of oil only are used, the matches appear poorer (Figures 16(a) and 16(b)). The reason again is that early in

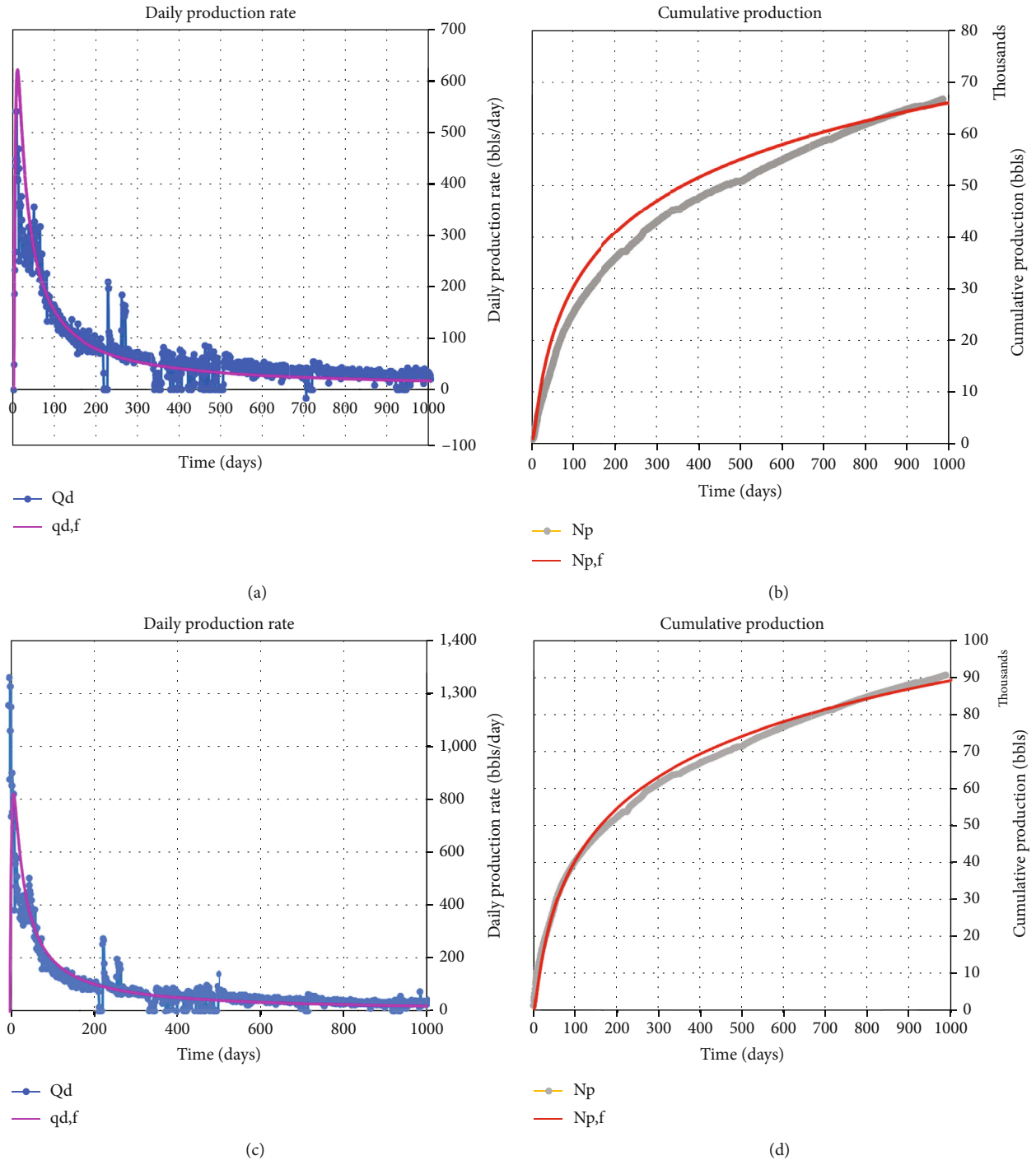

Figure 17: Well O: (a) Gaussian match on historic daily oil rate only; (b) corresponding match on cumulative oil production; (c) improved Gaussian DCA match on total fluid produced; (d) corresponding match on cumulative production data (total fluid).

the well life, there is significant water production (including some flowback water), such that matching oil rates with a single diffusivity throughout the well life results in poorer matches (Figure 16(a)).

Figures 17(a)–17(d) show the history matches for Well O. Using total daily fluid rates leads to improved Gaussian DCA matches of the historic production data (Figures 17(c) and 17(d)). However, if oil rates only are used, poorer matches appear (Figures 17(a) and 17(b)).

In a final check, history-matched well rates, generated with CMG-IMEX, were matched with the Gaussian method (Figure 18). Although the simulator data are free from operational noise, simulator history matches are nonunique and should therefore never be taken as more reliable than field production data. The CMG simulations cannot account for all the water production such as resulting from flowback. The main focus of such simulations is on the oil rate performance. Using the CMG best fit of oil rate only for Well H1, the

Table 4: Hydraulic diffusivities obtained for the history matches of Wells H1, M, R, and O (Figures 14–17).

Well name	Oil only (ft^2/day)	Oil only (m^2/s)	Total fluid (ft^2/day)	Total fluid (m^2/s)
H1	0.02362	2.54×10^{-8}	0.02340	2.52×10^{-8}
M	0.02450	2.63×10^{-8}	0.02376	2.56×10^{-8}
R	0.02278	2.45×10^{-8}	0.02230	2.40×10^{-8}
O	0.02580	2.77×10^{-8}	0.02500	2.69×10^{-8}

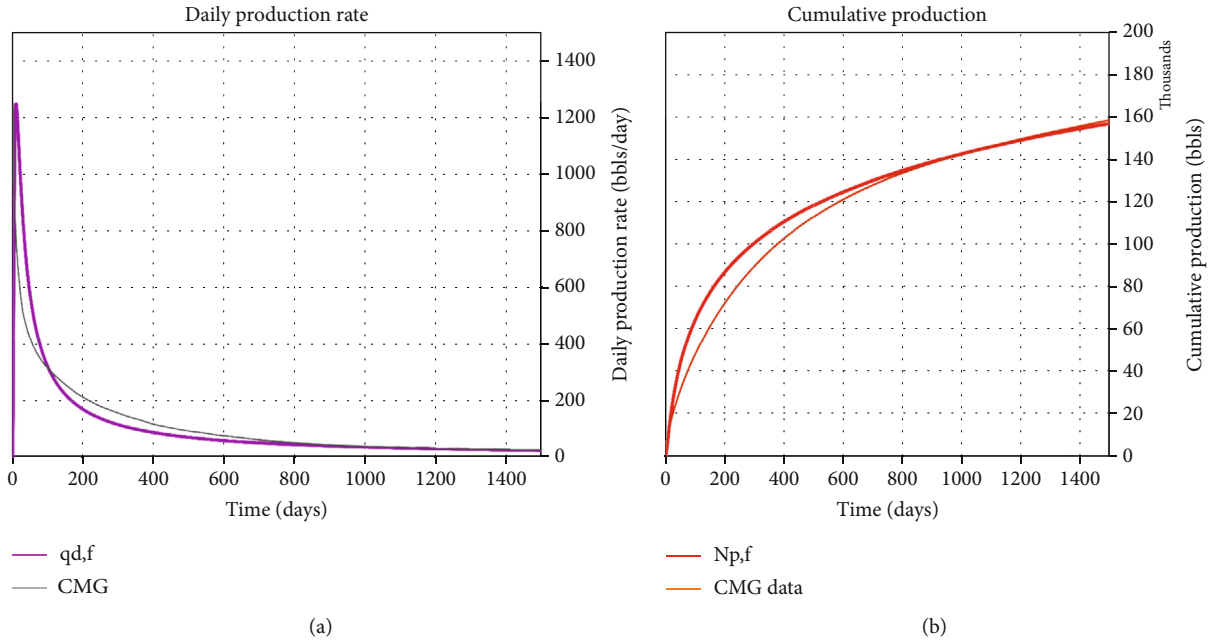

Figure 18: Well H: (a) Gaussian match on CMG history-matched daily oil rate only; (b) corresponding match on CMG output of cumulative oil production (oil only).

fit with Gaussian DCA gives again rather poor history (Figure 18). However, the Gaussian DCA invariably gives excellent fits to real well data, provided total fluid rates are used. Figures 14–17 give a good sense of the systematic error that may arise if only oil rate data is used. Figures 14–17 also give a good sense of the systematic error that may arise. Comparing the results of Figures 14 and 18 reveals the relative offsets. One take away from doing this check is that using CMG oil-only output for benchmarking the Gaussian method may be misleading. One should not doggedly try to match every aspect of the CMG curves. Besides, the CMG simulation used a black oil assumption due to which some minor multiphase flow effects also may affect the production rate output from the simulator platform.

In conclusion, it appears that history matching with Gaussian DCA of the oil rates only and using a single diffusivity throughout the well life, for all of the four wells analyzed as well as using CMG simulator output, results in poorer matches (especially for the early rate data) (Figures 14(a) and 14(b)–17(a) and 17(b) and 18). However, if the total fluid production is used, as recommended here, the Gaussian DCA appears to match the historic real well data with reasonable certainty (Figures 14(c) and 14(d)–17(c) and 17(d)). For the CMG simulation, only a constant water-cut ratio was used, so attempts to Gaussian match oil plus water rates from the simulator will not improve the results of Figure 18.

For the estimation of oil reserves with the Gaussian DCA method, the following procedure is recommended. First, for shale wells producing liquids, one should apply the Gaussian DCA method to history match the total fluid production, which will give excellent matches. Next, one can obtain the remaining oil reserves to be produced from a given day forward, by prorating the forward production (based on total fluid rate matches) for water-cut ratio, which then gives reserve estimations with the SEC-required reasonable certainty. For dry gas wells, the water production will be negligible, and excellent matches have been obtained using gas rates only [19].

Data Availability

No data or code will be made available with this paper.

Conflicts of Interest

The author declares that there are no conflicts of interest.

Acknowledgments

The author acknowledges the generous support provided by the College of Petroleum Engineering & Geosciences (CPG) at King Fahd University of Petroleum & Minerals (KFUPM). Dr. Ibere Alves (TAMU) gave valuable advice on choke effects and flow assurance. Dr. Fatih Tugan (TPAO) kindly availed the detailed analysis of Figure 9.

References

[1] J. Miskimins, *Hydraulic Fracturing: Fundamentals and Advancements*, Society of Petroleum Engineers, Richardson, TX, USA, 1st edition, 2019.

[2] M. F. Tugan and R. Weijermars, "Searching for the root cause of shale well rate variance: highly variable fracture treatment response," *Journal of Petroleum Science and Engineering*, vol. 210, article 109919, 2022.

[3] A. Nandlal and R. Weijermars, "Shale well factory model reviewed: Eagle Ford case study," *Journal of Petroleum Science and Engineering*, vol. 212, article 110158, 2022.

[4] R. Weijermars, A. Johnson, J. Denman, K. Salinas, and J. Williams, "Creditworthiness of North American oil companies and minsky effects of the (2014-2016) oil price shock," *Journal of Finance and Accounting*, vol. 6, no. 6, pp. 162–180, 2018.

[5] SPEE, "Monograph 3. Guidelines for the practical evaluation of undeveloped reserves in resource pays," Society of Petroleum Evaluation Engineers, Houston, TX, USA, 2010, https://spee.org/sites/spee.org/files/Monograph%203%20Errata.pdf.

[6] SPEE, *Monograph 4. Estimating Ultimate Recovery of Developed Wells in Low-Permeability Reservoirs*, SPEE, Houston, TX, USA, 2016, https://www.dropbox.com/s/sd2iljfvxoxjtgw/monograph-4-errata.pdf?dl=0.

[7] B. Chen, B. R. Barbosa, Y. Sun et al., "A review of hydraulic fracturing simulation," *Archives of Computational Methods in Engineering*, vol. 29, no. 4, pp. 1–58, 2022.

[8] Q. Feng, S. Xu, X. Xing, W. Zhang, and S. Wang, "Advances and challenges in shale oil development: a critical review," *Advances in Geo-Energy Research*, vol. 4, no. 4, pp. 406–418, 2020.

[9] S. D. Mohaghegh, "Reservoir modeling of shale formations," *Journal of Natural Gas Science and Engineering*, vol. 12, pp. 22–33, 2013.

[10] SPE Taskforce, *Final Report Unconventional Reserves Task Force*, The Woodlands, TX, USA, 2016(accessed on 21 March 2020), https://www.spwla.org/Documents/SPWLA/TEMP/Unconventional%20Taskforce%20Final%20Report.pdf.

[11] Y. Hu, R. Weijermars, L. Zuo, and W. Yu, "Benchmarking EUR estimates for hydraulically fractured wells with and without fracture hits using various DCA methods," *Journal of Petroleum Science and Engineering*, vol. 162, pp. 617–632, 2018.

[12] P. Manda and D. B. Nkazi, "The evaluation and sensitivity of decline curve modelling," *Energies*, vol. 13, no. 11, p. 2765, 2020.

[13] C. Afagwu, S. Al-Afnan, R. Weijermars, and M. Mahmoud, "Multiscale and multiphysics production forecasts of shale gas reservoirs: new simulation scheme based on Gaussian pressure transients," *Fuel*, vol. 336, article 127142, 2023.

[14] R. Weijermars, "Diffusive mass transfer and Gaussian pressure transient solutions for porous media," *MDPI Fluids*, vol. 6, no. 11, p. 379, 2021.

[15] R. Weijermars, "Production rate of multi-fractured wells modeled with Gaussian pressure transients," *Journal of Petroleum Science and Engineering*, vol. 210, article 110027, 2022.

[16] P. A. Slotte and C. F. Berg, "Lecture notes in well-testing," 2020, https://folk.ntnu.no/perarnsl/Literatur/lecture_notes.pdf.

[17] R. N. Horne, "Modern well test analysis. A computer aided approach," 1990, https://home.czu.cz/storage/575/52485_Ronald-N-Modern-Well-Test-Analysis.pdf.

[18] R. Weijermars, "Gaussian decline curve analysis of hydraulically fractured Wells in shale plays: examples from HFTS-1 (hydraulic fracture test site-1, Midland basin, West Texas)," *MDPI Energies*, vol. 15, no. 17, p. 6433, 2022.

[19] R. Weijermars and C. Afagwu, "Hydraulic diffusivity estimations for US shale gas reservoirs with Gaussian method: implications for pore-scale diffusion processes in underground repositories," *Journal of Natural Gas Science and Engineering*, vol. 106, article 104682, 2022.

[20] C. Cipolla, C. Gilbert, A. Sharma, and J. LeBas, *Case History of Completion Optimization in the Utica*, Society of Petroleum Engineers, Houston, TX, USA, 2018.

[21] G. Fowler, M. McClure, and C. Cipolla, "A Utica case study: the impact of permeability estimates on history matching, fracture length, and well spacing," in *Proceedings of the SPE Annual Technical Conference and Exhibition*, pp. 1–12, Calgary, AB, Canada, 2019.

[22] R. Weijermars, K. Nandlal, A. Khanal, and M. F. Tugan, "Comparison of pressure front with tracer front advance and principal flow regimes in hydraulically fractured wells in unconventional reservoirs," *Journal of Petroleum Science and Engineering*, vol. 183, article 106407, 2019.

[23] R. Weijermars, A. van Harmelen, L. Zuo, I. Nascentes Alves, and W. Yu, "High-resolution visualization of flow interference between frac clusters (part 1): model verification and basic cases," in *Proceedings of the 5th Unconventional Resources Technology Conference*, pp. 1–18, Austin, TX, USA, 2017.